Time characteristics of electron, muon, and Cherenkov photon fronts in giant air showers

A. M. Anokhina,[1] L. G. Dedenko,[2] G. F. Fedorova,[1] V. I. Galkin,[2] N. Inoue,[3] A. Misaki,[4] S. N. Nazarov,[2] and T. M. Roganova[1]

[1]*Skobel'tsyn Institute of Nuclear Physics, Moscow State University, 119899 Moscow, Russia*

[2]*Department of Physics, Moscow State University, 119899 Moscow, Russia*

[3]*Department of Physics, Saitama University, 338 Urawa, Japan*

[4]*National Graduate Institute for Policy Studies, Saitama University, 338 Urawa, Japan*

(Received 27 January 1997; revised manuscript received 1 June 1998; published 28 June 1999)

Calculations of the space-time structure of giant air showers in the energy range 10^{17}–10^{21} eV carried out in the framework of the quark-gluon string model show the existence of three separate disks (or better lenses) of muons, Cherenkov photons, and electrons which follow each other. In a shower with an energy of 10^{19} eV time delays at 1000 m from the shower core can be as large as 420, 450, and 1120 ns for muons, Cherenkov photons, and electrons, respectively, while the disk thickness for these three components can reach the values of 500, 680, and 1160 ns, respectively. At larger core distances the time delay and disk thickness may exceed a few μs and should be taken into account both in designing the new array electronics and interpreting the experimental data. Highly inclined showers which consist mainly of muons display a much flatter front: time delay decreases down to about 110 ns at a distance of 1000 m from the shower core. Approximations of the time parameters dependence on the primary energy and core distance are presented. The measurements of electron, muon, and Cherenkov photon time pulses are suggested to improve the estimations of the arrival direction and the energy of the showers and also to study the primary particle composition and parameters of hadron interactions at energies above 10^{19} eV. [S0556-2821(99)06411-5]

PACS number(s): 96.40.Pq, 96.40.De

I. INTRODUCTION

The first detection of a giant air shower (GAS) by Linsley [1] followed by observations at Haverah Park [2,3] and Sydney [4,5] put forward a very important puzzle of sources of primary cosmic rays of energies up to 10^{20} eV. This puzzle may be connected with the most fundamental problems of particle physics and astrophysics such as the existence of elementary particles with masses of 10^{25}–10^{28} eV [6], topological defects [7], unknown phenomena in active galactic nuclei, etc.

The interactions between the primeval microwave photons and cosmic ray protons (or nuclei) cause serious energy losses and, as a result, a sharp drop in the flux of cosmic rays at an energy of 3×10^{19}–6×10^{19} eV [8,9]. This prediction of the Greizen-Zatsepin-Kuzmin (GZK) cutoff and new observations of the GAS at Yakutsk [10], AGASA [11], and Utah [12] make the puzzle of the most energetic cosmic rays even more dramatic. If the extragalactic origin of cosmic rays is assumed then the distant sources are ruled out and we have to search for very powerful phenomena which may accelerate particles up to an energy of 10^{21} eV (or even more) within 30–50 Mpc or superheavy massive particles [13].

To investigate this very intriguing mystery of superhigh energy cosmic rays some new projects were suggested [14–16]. These new arrays have to have large spacings between detectors to cover a huge area of thousands of square kilometers at reasonable cost. So it is inevitable to take the detector responses at distances above 1 km from the shower core into account. It is of primary importance to estimate correctly both energy and arrival direction of giant showers. Thus calculations of characteristics and time parameters of giant showers up to distances of a few kilometers from the shower core should be carried out. These calculations may be used both in elaborating electronics of new arrays and interpreting the experimental data. In this paper we present the results of calculations of time delays and shower disk thicknesses for electrons, muons, and Cherenkov photons up to distances of about 5 km in the energy range of 10^{17}–10^{21} eV.

II. METHOD OF CALCULATION

Calculations were carried out in the framework of the quark-gluon string (QGS) model [17] for primary protons and observation level of 920 g/cm^2 both for vertical and inclined showers with a zenith angle of 60°. Neutral pion interactions with nuclei in the atmosphere were taken into account at proton energies above 10^{19} eV. The Migdal cross sections for pair production and bremsstrahlung processes [18] were used to calculate the electron-photon shower development with the Landau-Pomeranchuk-Migdal (LPM) effect included at high energies. The hybrid method [19] was used to estimate both mean values and standard deviations of considered parameters. This method enables us to account for fluctuations of number and points of interactions in the atmosphere and energy releases of primary protons using a Monte Carlo procedure while the development of cascades from numerous charged pions is considered on average by a step-by-step approach [20] (for some details see Appendix A).

The exact estimations of time parameters for an electron component of showers are rather complicated due to the Coulomb scattering which can be solved in principle by the Monte Carlo method [21]. We suggest to use some approximations. The first one enables us to calculate with reasonable accuracy mean time delay τ and the disk thickness σ for the electron disk. The method of calculation used enables us to

 ©1999 The American Physical Society

know the production height h_γ of every gamma quantum of energy E_γ born in a shower. Thus one can directly estimate the height h where this particular electron-photon shower reaches its maximum and calculate the time delay at distance R from the shower core

$$t=\frac{h}{c}[\sqrt{1+(R/h)^2}-1]. \tag{1}$$

Here c is the speed of light and h is a function of h_γ and E_γ. Averaging over all gamma quanta produced in an extensive air shower (EAS) we can find an estimate of mean time delay:

$$\tau=\frac{\int t\rho_e(E_\gamma,h_\gamma,R)F_\gamma(E_\gamma,E_0,h_\gamma)dE_\gamma dh_\gamma}{\int \rho_e(E_\gamma,h_\gamma,R)F_\gamma(E_\gamma,E_0,h_\gamma)dE_\gamma dh_\gamma}. \tag{2}$$

Here $F_\gamma(E_\gamma,E_0,h_\gamma)$ is the energy spectrum of gamma quanta produced at height h_γ in a shower of energy E_0 and $\rho_e(E_\gamma,h_\gamma,R)$ is Nishimura-Kamata-Greisen function (NKG) [22]. Substituting t in Eq. (2) with t^2 one can find an estimate for $\langle\tau^2\rangle$. Then the disk thickness can be calculated as

$$\sigma=\sqrt{\langle\tau^2\rangle-\tau^2}. \tag{3}$$

The second approximation gives very lower limits for both τ and σ. It utilizes the height h_γ in Eq. (1) instead of h. The upper limit for time delay seems to be R/c.

One should remember that both approximations give only some limits for time delay τ and disk thickness σ because electrons may come to a detector, situated at core distance R, from any point of the shower and their trajectory is not a straight line but a zigzag curve due to Coulomb scattering. Nevertheless, estimates (2) and (3) can serve as reasonable guides for the time delay and disk thickness of the electron component of EAS in the case of the first approximation.

The procedure of time parameter estimation is much more straightforward for muons. In this case instead of Eq. (1) we can write

$$t=\frac{h_\mu}{c}\left[\frac{1}{\beta}\sqrt{1+(R/h_\mu)^2}-1\right]. \tag{4}$$

Here β is the speed of muon of energy E_μ and h_μ is its production height. Then one should use formulas (2) and (3) on substituting ρ_e and F_γ by muon lateral structure function ρ_μ and muon source function F_μ, correspondingly, which are calculated in every shower in an assumption that the muon spread at the detector plane is approximately described in terms of the effective transverse momentum distribution of produced pions:

$$f(p_t)dp_t=p_t/p_0^2\exp(-p_t/p_0)dp_t. \tag{5}$$

Here p_0 is equal to 0.2 GeV/c. The threshold energy of muons was assumed to be $0.5\sec\theta$ GeV, here θ is the zenith angle of a shower axis. A detailed discussion on the choice of parameters and on the validity limits of Eq. (5) is given in Appendix B.

It should be pointed out that the suggested procedure (1)–(4) to estimate τ and σ both for electrons and muons saves computing time. The electron and muon time pulses may also be approximately estimated in a similar way (see Appendix C).

Cherenkov light time characteristic estimations were based on average shower light pulse calculations [23]. One can express the pulse shape of Cherenkov light emitted by average air shower, initiated by primary particle of energy E_0, and received by a detector at core distance R as (in detector bound spherical coordinate system)

$$\frac{dQ(E_0,R,T)}{dT}=\int_0^{2\pi}d\psi\int_0^{\chi_{\max}}\sin\chi d\chi \times\int_{E_{\rm thr}(r,\chi)}^{E_0}dE\,B(E,\vec{r},\Delta\lambda)C(\vec{r},\Delta\lambda) \times P(E_0,E,\vec{r})\frac{dr(\chi,\psi,T)}{dT}. \tag{6}$$

Here $\vec{r}=(r,\chi,\psi)$ is the radius vector of spherical coordinate system bound to detector, $B(E,\vec{r},\Delta\lambda)$ is the number of Cherenkov photons emitted by a charged particle of energy E in wavelength band $\Delta\lambda$ per unit length in the air, and $C(\vec{r},\Delta\lambda)$ is the air transmission coefficient; then

$$P(E_0,E,\vec{r})=\int d\vec{\theta}\,P[E_0,E,t(\vec{r}),\vec{r}(R,\vec{r},\vec{\theta}),\vec{\xi}(\vec{r},\vec{\theta})] \times\delta(|\vec{\theta}-\vec{\theta}_c(h,E)|). \tag{7}$$

Here $P(E_0,E,t,\vec{r},\vec{\xi})$ is the differential in energy electron spatial-angular distribution function in average air showers initiated by primary proton, $\vec{r},\vec{\xi}$ are the two-dimensional lateral and angular coordinates in the shower bound system, $\chi_{\max}$ is the detector cone half angle, $\theta_c(h,E)$ is the Cherenkov angle in air, h is the height above sea level, and $E_{\rm thr}$ is the Cherenkov radiation threshold energy.

Integration in Eq. (6) is carried out over the shower secondary electron energy E and the so-called equal delay surface. This is the set of points in space from which the Cherenkov photons that reach simultaneously a detector are emitted, i.e., show one and the same time delay T relative to the moment when the most energetic shower electrons hit the detector array.

III. RESULTS AND DISCUSSION

A. The space-time structure of giant showers

The main goal of present calculations is to shed more light on the space-time structure of giant showers. A simple formula for time delay (and disk thickness), suggested by Linsley [24], is well known,

$$\tau=a(1+R/30m)^b,\quad ns. \tag{8}$$

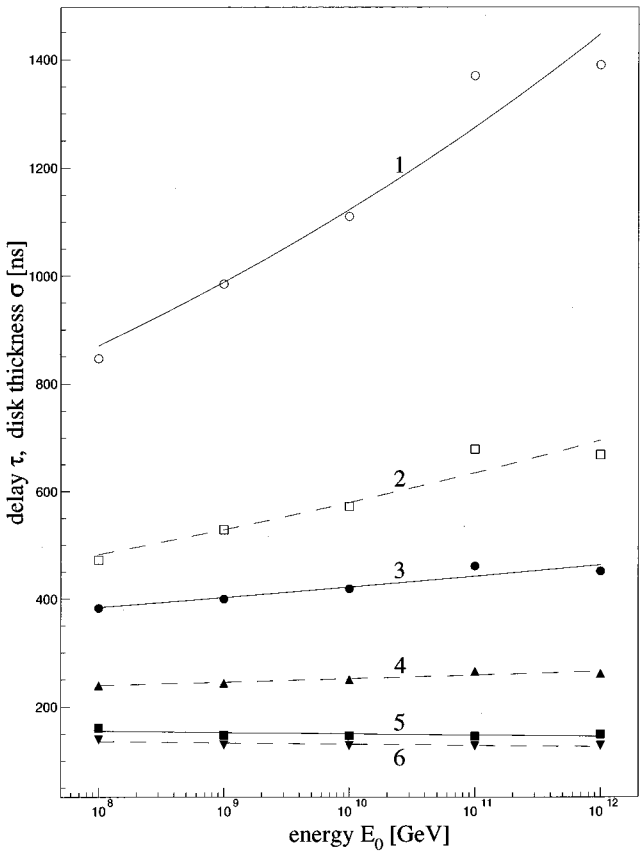

FIG. 1. Dependence of mean time delay τ (solid curves) and disk thicknesses σ (dashed curves) on energy E_0 at 1000 m from the shower core for vertical showers. Curves 1, 2 correspond to electrons in the first approximation (see text), curves 3, 4 stand for muons, curves 5, 6 designate electrons in the second approximation.

Here $a=2.6$, $b=1.5$, and R is the core distance in meters. This formula with some corrections proved to be adequate in some investigations [25,26] but explicit dependence of its parameters a and b on the energy E_0 and the nature of the primary particle and also on the zenith angle θ at which the shower arrived have never been given. It is obvious that the depth of shower maximum approaches the observation level as the primary energy increases. Thus the time delay should also slowly increase with primary energy. Our calculations confirm this conclusion (see also Ref. [27]). Figure 1 displays time delay τ (solid curves) and disk thickness σ (dashed curves) at a distance of 1000 m from the shower core (the most typical value for new arrays) for electrons for both approximations used (curves 1, 2 are the first approximation and curves 5, 6 are the second one) and muons (curves 3,4) versus energy E_0 of primary protons in vertical showers. Curve 1 for the electron disk shows clearly an increase with E_0 while the second approximation (curve 5) displays a constant value because the production heights of high energy neutral pions depend on E_0 very slightly due to the nature of hadron interactions. Curve 3 for the muon disk also shows a pronounced increase with E_0 due to the shift of shower maximum of the low energy hadron component of the shower toward the level of observation. To find the explicit dependence of time parameters on E_0 one can approximate curves 1, 2 and 3, 4 by the simple formula

$$\tau = \alpha (E_0/10^{19}\ \text{eV})^{\beta}. \tag{9}$$

Coefficients α and β are listed below in Table I both for the mean time delay τ and disk thickness σ with uncertainty of 20%.

TABLE I. Approximation (9) coefficients for τ and σ at $R=1000$ m.

	Electron		Muon		Cherenkov light
Parameter	0^0	60°	0°	60°	0°
			Time delay		
α	1120.0	320.0	420.0	110.0	450.0
β	0.0552		0.0203	0.0224	0.0210
			Disk thickness		
α	580.0	300.0	250.0	54.0	340.0
β	0.0395		0.0113	0.024	0.0227

Monte Carlo calculations [21] were carried out at an energy of 10^{14} eV up to core distance of 700 m. It is worth noting that if the results of Ref. [21] on time delay and disk thickness for electrons and muons are extrapolated to distance $R=1000$ m then they coincide with estimates according to formula (9), extrapolated to 10^{14} eV, within an uncertainty of a few per cent with the exception of the muon disk thickness which is by a factor of about 1.5 lower possibly due to the hadron-hadron interaction model used in Ref. [21]. As the scaling is mildly violated in the fragmentation region and significantly violated in the central region at energies above 10^{12} eV [21], a large number of pions are produced at the very beginning of hadron cascade development and thus small fluctuations are expected. Thus a simple approximation formula (9) seems to be valid for time delay and disk thickness both for electrons and muons within a huge range of energy from 10^{14} to 10^{21} eV at distance $R \simeq 1000$ m.

Curves 5 and 6 can serve as very low limits for electron time delay and disk thickness because the second approximation takes into account only the production on heights h_γ of all gamma quanta produced in the decay of neutral pions, disregarding electron cascade development.

The time delay and disk thickness for Cherenkov photons are also increasing with energy E_0 as one can see in Fig. 2. Curves 1, 2, and 3 display time $t_{\max}$ of a pulse maximum, median time t_{med}, and mean time t_{cm}, respectively, at a core distance of 1000 m. Curve 4 shows the full width at half maximum (FWHM) $t_{1/2}$ of the Cherenkov pulse. The approximation formula (9) coefficients for t_{cm} and $t_{1/2}$ can be found in Table I.

Thus a very interesting time-space picture of a vertical shower may be drawn. In a shower with the energy of 10^{19} eV first particles to arrive at detector plane at core distance of 1000 m are muons which come about 420 ns later than imaginary high energy particles moving at the speed of light along the shower axis. The standard muon disk thickness, determined by Eq. (3) is about 250 ns. Then Cherenkov

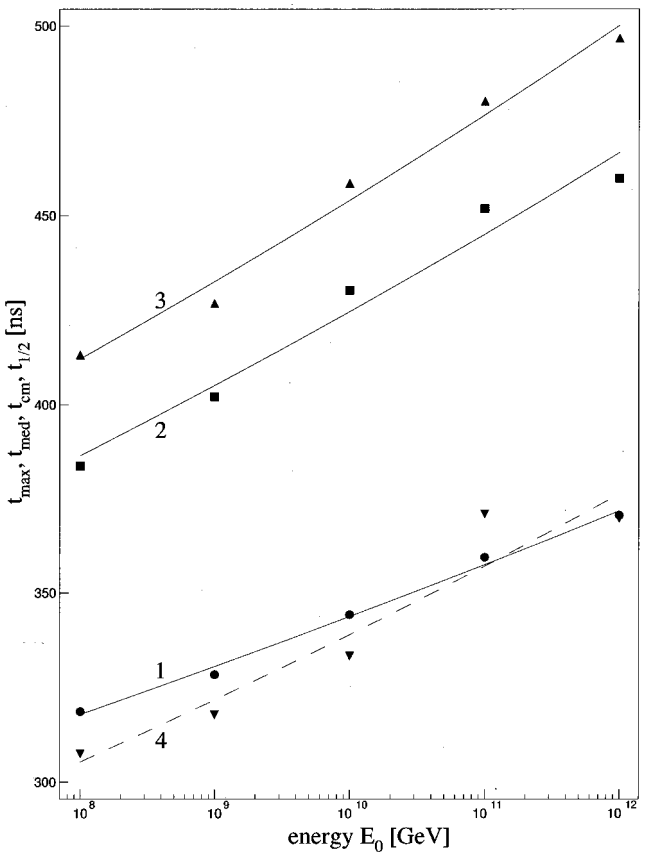

FIG. 2. Dependence of Cherenkov pulse maximum time $t_{\max}$ (curve 1), median time t_{med} (curve 2), mean time t_{cm} (curve 3), and FWHM $t_{1/2}$ (curve 4) on energy E_0 at 1000 m from the shower core for vertical showers.

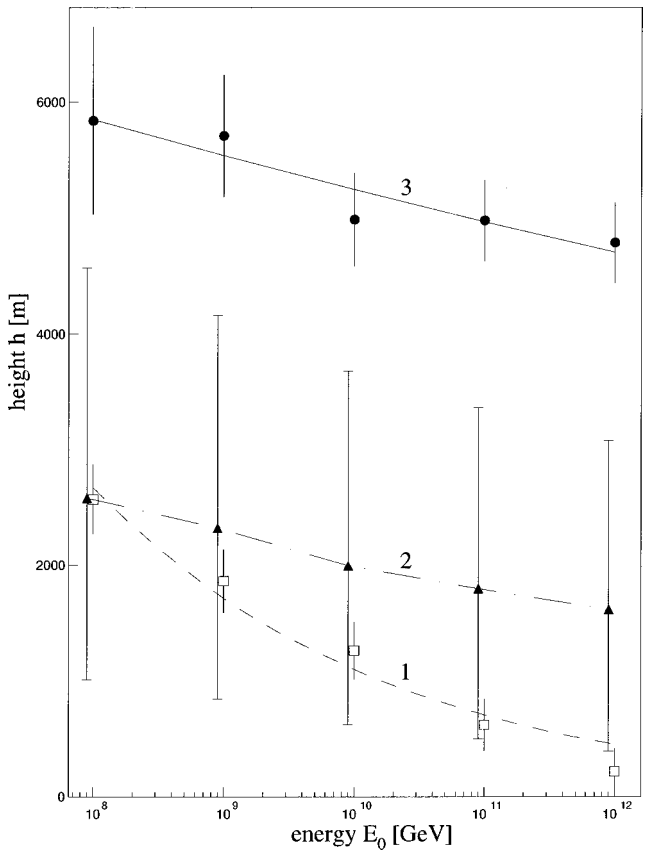

FIG. 3. Dependence of production heights for electrons (curve 1), Cherenkov photons (curve 2), and muons (curve 3) on energy E_0 for vertical showers.

photons hit this plane about 30 ns later with a full width of 340 ns. At last, electrons with an additional 670 ns delay and standard disk thickness of 580 ns come. So three ''independent'' rather thick disks (or better ''lenses'') of muons, Cherenkov photons, and electrons follow each other with a certain delay to strike the detector plane. Such a structure of the shower front can be understood with the help of Fig. 3 which displays mean production heights for electrons (curve 1) and Cherenkov photons (curve 2) versus E_0. Curve 3 shows the median production height dependence on energy E_0 for muons. The bars display the effective widths related to production regions.

It is remarkable that muons are produced higher in the atmosphere than Cherenkov photons as can be seen in Fig. 3. Electrons are gathered from a rather close vicinity of the detector plane. Thus at a core distance of 1000 m electrons have to have a noticeable inclination towards vertical. In general the height of production may be estimated with the help of the known time delays presented in Table I by the simple formula

$$h = 0.5\tau c[(r/\tau c)^2 - 1], \quad m, \tag{10}$$

which is well confirmed by the exact calculations shown in Fig. 3. So time delays and production heights are closely correlated.

As time parameters increase with growing the energy E_0 particle detector stations of a giant array should be able to gather electrons and muons or the Cherenkov photons for a few μs due to both the large time delay and large disk thickness at core distances of about 1 km. Then, to complete the picture, we have to say that hadrons are concentrated near the shower axis and scintillation photons are important at distances over a few km from the shower core and will be considered in a separate paper.

Then it is important to notice that electrons in strongly inclined showers are absorbed and the only detectable particles are muons and the Cherenkov photons. Figure 4 shows mean time delay τ (solid curve) and disk thickness σ (dashed curve) for muons as a function of energy E_0 of primary protons for inclined showers with a zenith angle of 60° at core distance of 1000 m. One can see a profound decrease of time delay τ and disk thickness σ due to effective increase of production height but again time τ is increasing with energy E_0. Coefficients of approximation (9) for inclined showers are also listed in Table I.

For arrays with widely spaced detector stations, and vertical showers of energy 10^{20} eV, Fig. 5 shows the most important dependencies of time delay (solid lines) and disk thickness (dashed lines) as a function of the distance R from shower core, both for electrons (curves 1 and 2) and for muons (curves 3 and 4). Curves 5 and 6 serve as very low limits for electrons in the second approximation used. The

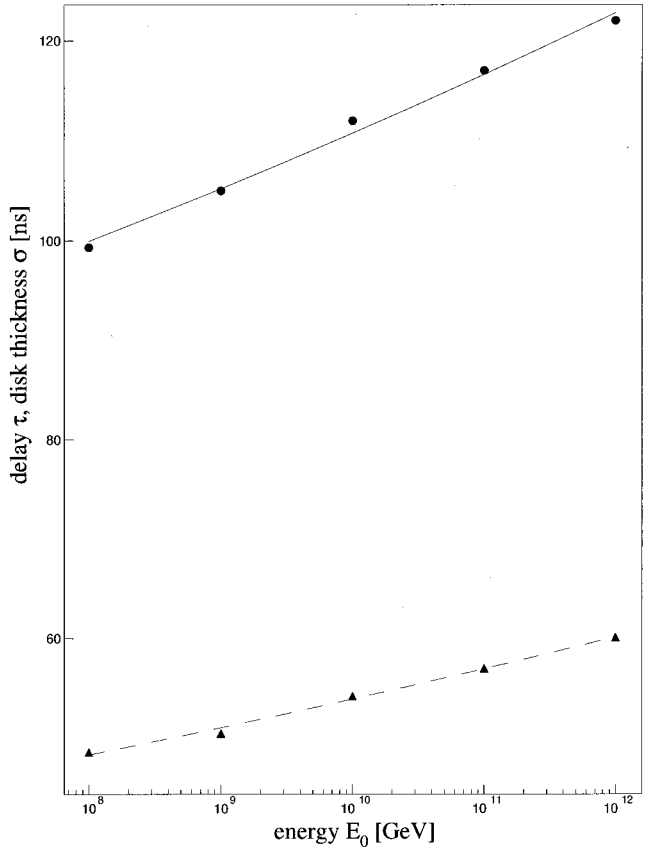

FIG. 4. Dependence of mean time delay τ (solid curve) and disk thickness σ (dashed curve) on energy E_0 for muons in inclined showers with the zenith angle of 60°.

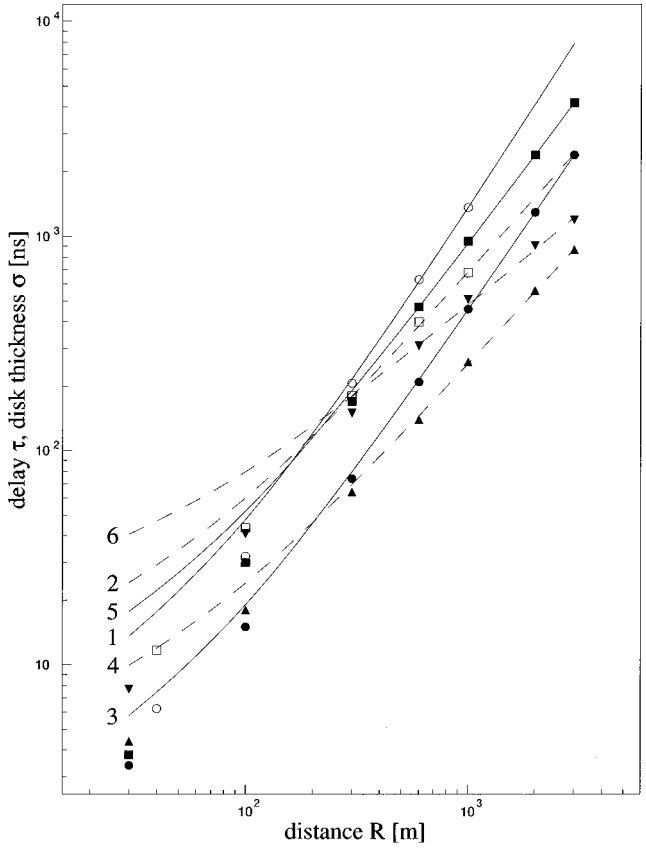

FIG. 5. Dependence of mean time delay τ (solid curves) and disk thickness σ (dashed curves) on core distance R for electrons (curves 1, 2 correspond to the first approximation, curves 5, 6 correspond to the second one) and muons (curves 3, 4) in vertical showers with the energy 10^{20} eV.

first thing to notice is a huge time delay of 10 μs at distances of 4–5 km from the shower core and a comparable disk thickness. The second important feature that should be mentioned is a large divergence of coefficients a and b, used in formula (8) to approximate dependencies shown in Fig. 5 from parameters given by Linsley ($a=2.6$; $b=1.5$). This divergence may also be observed at a energy of 10^{14} eV [21]. Table II shows coefficients a and b for energies of 10^{14} eV [21] and 10^{20} eV (Fig. 5) for both the vertical and inclined showers. We note only that coefficient a for electrons at an energy of 10^{20} eV is about a factor 2 larger than Linsley's parameter and about twice less at energy of 10^{14} eV [21] with exponents b also being different. Deviations of parameters a and b from the Linsley's parameters are even more dramatic for inclined showers (see below). In addition to this, the simple approximation (8) seems not to be valid at distances $R \leqslant 100$ m.

So, an important conclusion to be made is that coefficients a and b in approximation (8) depend strongly on energy E_0 of the shower and on the zenith angle θ. Thus these dependencies should be taken into account in order to correctly interpret data.

Figure 6 displays the radial dependencies of time delays $t_{\max}$, t_{med}, and t_{cm} (curves 1, 2, and 3, respectively) and FWHM $t_{1/2}$ (curve 4) for the Cherenkov light pulses for vertical showers of energy 10^{20} eV. These dependencies are multiplied by a factor of $(30/R)^2$ to clearly show the differences between curves. Again a huge time delays and disk thickness of Cherenkov photons of the order of a few μs should be pointed out at distances of 4–5 km. Parameters of approximation (8) for curves 2 and 4 are also listed in Table II.

In the case of inclined showers with a zenith angle of 60° and an energy of 10^{20} eV, Fig. 7 shows the time delay (solid curve) and disk thickness (dashed curve) for electrons (curves 1, 2) and for muons (curves 3, 4) versus the lateral distance R. The corresponding parameters a and b are also

TABLE II. Approximation (8) coefficients.

	Electron			Muon			Cherenkov light
Parameter	0°		60°	0^0		60°	0°
	Time delay						
E_0,eV	10^{14}	10^{20}	10^{20}	10^{14}	10^{20}	10^{20}	10^{20}
a	1.28	4.33	0.299	0.74	2.50	0.272	1.65
b	1.72	1.63	1.89	1.66	1.48	1.73	−0.359
	Disk thickness						
a	2.00	10.7	2.26	1.65	5.34	0.377	1.76
b	1.44	1.18	1.34	1.25	1.11	1.44	1.45

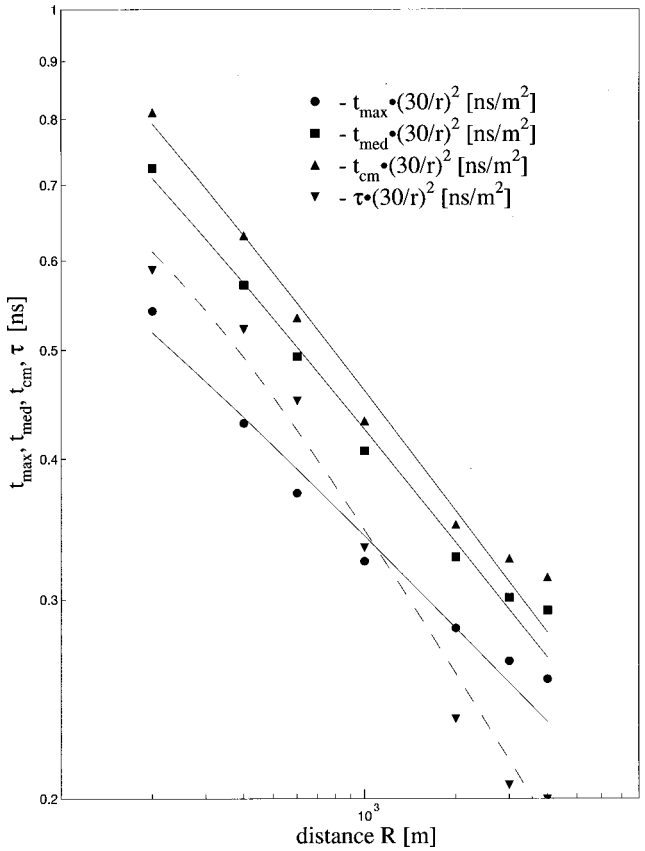

FIG. 6. Dependence of Cherenkov pulse maximum time $t_{\max}$ (curve 1), median time t_{med} (curve 2), mean time t_{cm} (curve 3), and FWHM $t_{1/2}$ (curve 4) multiplied by a factor of $(30\ \mathrm{m/R})^2$ on core distance R for vertical showers with the energy 10^{20} eV.

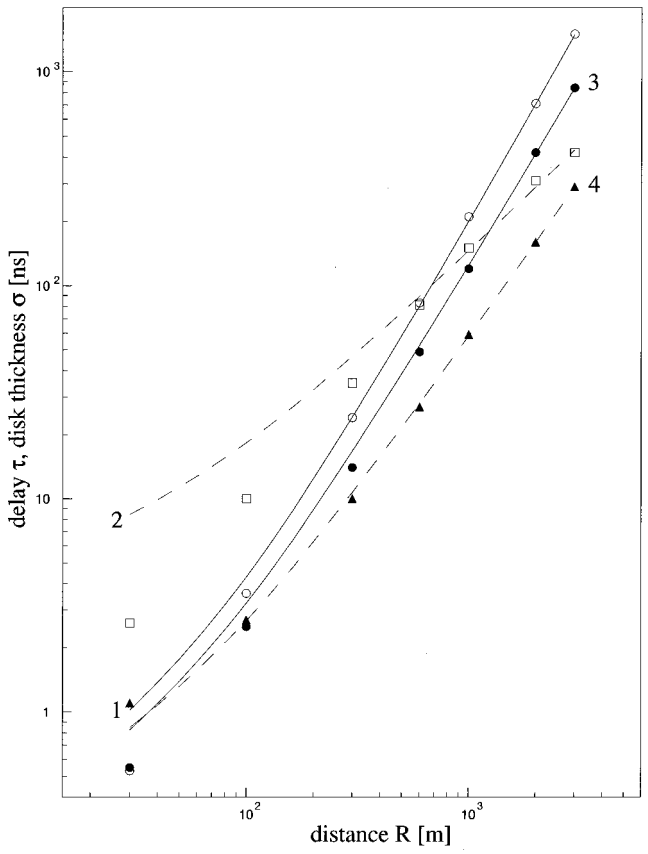

FIG. 7. Mean time delay τ (solid curves) and disk thickness σ (dashed curves) for electrons (curves 1, 2, first approximation) and muons (curves 3, 4) versus core distance R in inclined showers with the zenith angle 60° and energy 10^{20} eV.

listed in Table II. An important conclusion follows from the data presented in Table II. Coefficient a and exponent b strongly depend on zenith angle θ. Thus dependencies of a and b on both energy E_0 of primary protons and zenith angle θ should be taken into account. Table III shows an approximation of a and b dependence on E_0 using Eq. (9), δ substitutes α, γ substitutes β both for time delay and disk thickness at energies above 10^{19} eV with an uncertainty of 20%.

Figures 5–7 display the dependence of electron, muon, and Cherenkov photon disk thicknesses on the radial distance R from the shower core. So the time pulses measurements can provide an additional information in our effort to estimate the shower core location. These measurements are also of importance in determining the arrival direction of the primary particles because time parameters depend strongly on the zenith angle θ and thus also in estimating the energy E_0 of showers.

Finally these measurements for electrons, muons, and Cherenkov photons enable us to estimate the production height of different shower components and thus to draw some conclusions about the nature of primary particle or parameters of hadron interaction at superhigh energies.

Thus the time pulse measurements of different shower components may be suggested as a source of very important information about a giant shower. As an example Fig. 8 displays time Cherenkov pulses at a core distance of 1000 m for energies of 10^{17}, 10^{18}, 10^{19}, 10^{20}, and 10^{21} eV. One can clearly observe both the dynamics of pulse shape change with energy E_0 and the absolute level of signal to be detected.

B. The comparison with the experimental data

To display the reliability of the space-time structure of giant showers presented above calculations at lower energies near the shower axis may be compared with the available experimental data. The experimental data on particle average arrival time τ at energies 10^{15}–10^{17} eV and radial distances $R=200$–800 m for nearly vertical showers [28] were approximated by the formula (8) with coefficients $a=2.0\pm0.4$ ns and $b=1.69\pm0.07$ which should be compared with $a=2.3$ ns and $b=1.7$ from Table II for vertical showers. The approximation coefficients for the particle disk width FWHM $t_{1/2}$ were found as $a=4.2\pm0.8$ ns and $b=1.44\pm0.07$ [28], while the Table II gives $a\simeq4.0$ ns and $b\simeq1.4$ but for the disk thickness σ. So the results of calculations for the mean time delay fit the data [28] but as for the disk width the comparison is not so straightforward because of different values are approximated though the dependence on radial distance R and the width itself seem also to be comparable.

In Fig. 9 the average observed densities of muons per m^2 per 100 ns (black points) [29] and the MOCCA simulation

TABLE III. Approximation (9) coefficients for parameters a, b in Eq. (8).

Parameter	Electron		Muon				Cherenkov light	
	0°		0°		60°		0°	
	Time delay							
	δ	γ	δ	γ	δ	γ	δ	γ
a	2.74	0.113	2.29	0.0287	0.254	0.0279	1.55	0.078
b	1.70	−0.0122	1.49	−0.00173	1.74	−0.00125	1.44	0.009
	Disk thickness							
a	7.30	0.0968	4.63	0.0458	0.310	0.0638	1.52	0.032
b	1.24	−0.0132	1.13	−0.00888	1.48	−0.0086	−0.358	0.0027

results (solid line) presented in Ref. [29] are compared with the results of our calculations (open diamonds) at a core distance R of 1260 m in showers with the energy E_0 of 2×10^{18} eV. The experimental data and simulation results cannot be compared directly with each other because the first recorded particle in each observed shower is considered not to be delayed while we assumed the delay time to be zero for the moment then a particle moving with the speed of light along the shower axis strikes the detector plane. We have estimated the mean delay time as $\tau=780$ ns and the disk thickness as $\sigma=530$ ns, then some ''shift'' of the calculated distribution by $\delta=\tau-\sigma$ should be considered in comparing it to the data. In any case the shape of our distribution fits both the data [29] and the results of the MOCCA simulation well while the signal (total muon density) is 2 times less; this is a problem with the QGS model used. This difference by a factor of 2 can be explained as follows. Our calculations of muon densities should be multiplied by factor of 1.42 due to the calorimetry of showers carried out at the Yakutsk array [54] and a factor of 1.5 is the difference in energy estimations at the Yakutsk and the Akeno arrays. One more comment is that the electrons with energies above 40 MeV may contaminate the tail of the observed distribution while our calculations disregarded this effect. Figure 10 displays the electron delay time distribution (black points) and the MOCCA simulation results (solid line) presented in Ref. [29] to be compared with the results of our calculations (open diamonds in the modified NKG approximation [54] and open squares in the NKG approximation). As we have estimated with the help of the first approximation the mean delay time as $\tau=1200$ ns and the disk width as $\sigma=500$ ns so some ''shift'' of calculated distribution by $\delta=\tau-\sigma$ should be suggested to compare with the data. In this case the shape of

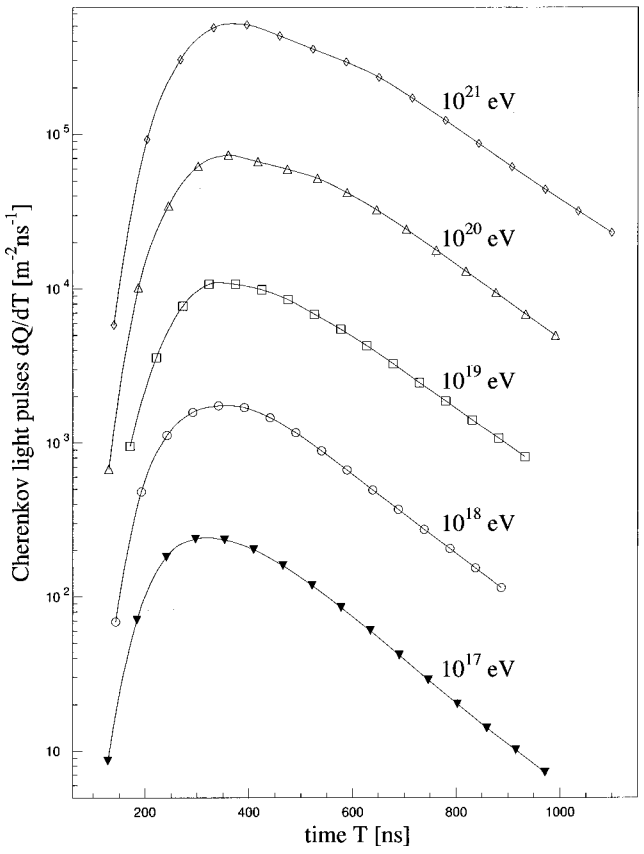

FIG. 8. Arrival time distributions for the Cherenkov photons in vertical showers with energies 10^{17}, 10^{18}, 10^{19}, 10^{20}, and 10^{21} eV at the core distance of 1000 m.

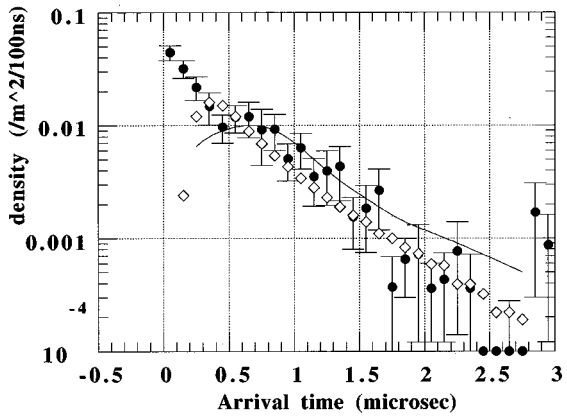

FIG. 9. Arrival time distributions for muons at the core distance of 1260 m in showers with the energy of 2×10^{18} eV. Points represent the data [29]. The first recorded particle in each shower is considered not to be delayed. The solid line is the expectation from simulations by the MOCCA code also taken from Ref. [29]. Diamonds are the result of the present simulations with the delay time accounted from the moment when the shower axis strikes the array plane.

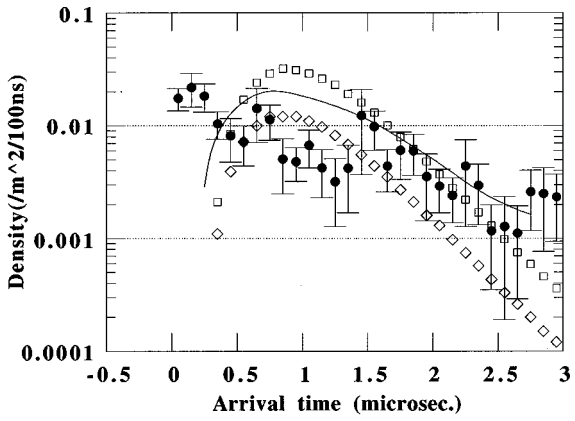

FIG. 10. Arrival time distributions for electrons at the core distance of 1260 m in showers with the energy of 2×10^{18} eV. Points represent the data [29]. The first recorded particle in each shower is considered not to be delayed. The solid line is the expectation from simulations by the MOCCA code also taken from Ref. [29]. Diamonds are the result of the present simulations with the delay time accounted from the moment when the shower axis strikes the array plane in case of the modified NKG approximation and open squares are also our results for the NKG approximation.

distributions is also comparable though the total signal is 2 times higher in the case of the MOCCA simulation and approximately 3 times higher in the case of the NKG approximation disregarding a contamination of the observed distribution by high energy photons. In the case of the modified NKG approximation the total signal seems to agree with the data [29].

The dependence of the average delay time on radial distance R was shown in Fig. 11 when 1, 4, and 10 particles hit the detector at the PeV energy region [30] together with the results of our calculations (open diamonds). Figure 12 illustrates the dependence of the half width at 70% peak level (HW70) on radial distance R. It is seen that at radial distances above 100 m our calculations for the primary proton with an energy of 3×10^{15} eV fit the data [30]. Probably only the full Monte Carlo simulation should be used to fit the data near the shower core.

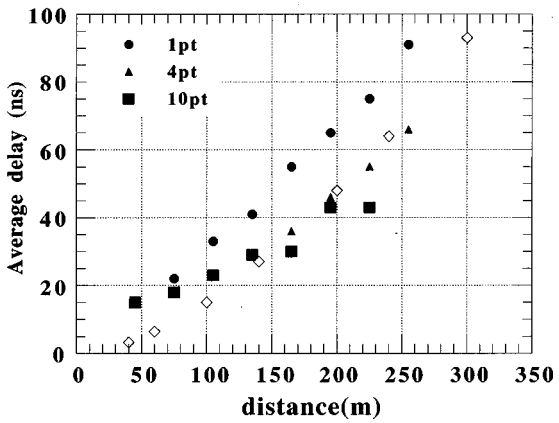

FIG. 11. Average time delays for electrons in showers versus radial distance in the PeV energy region. Points represent the data [30] when 1, 4, and 10 particle hit the detector. Diamonds are the present simulations of the average disk profile for the delay time accounted from the moment when the shower axis strikes the array plane.

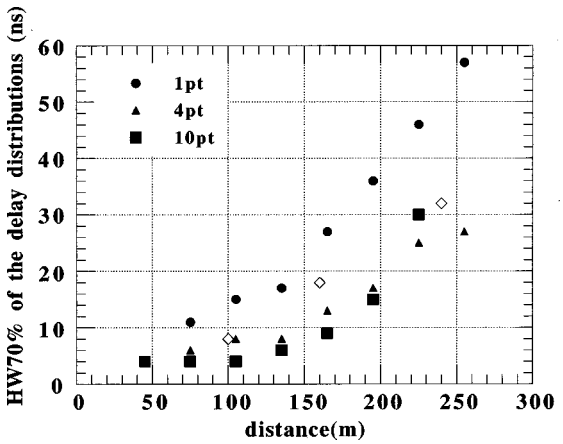

FIG. 12. The full width at 70% level (FW70) for electrons in showers versus radial distance in the PeV energy region. Points represent the data [30] when 1, 4, and 10 particle hit the detector. Diamonds are the present simulations of this full width for the delay time accounted from the moment when the shower axis strikes the array plane.

The measurements by the COVER-PLASTEX experiment embedded in the GREX surface array at Haverah Park gave a mean time delay of $\tau=22$ ns and a disk width of $\sigma=35$ ns [31] and after taking into account systematic errors these values have been presented as $\tau=28$ ns and $\sigma=40$ ns at a distance $R=100$ m from the shower core in the PeV energy region. Our calculations for this distance gave $\tau=17$ ns and $\sigma=29$ ns at $E_0=10^{14}$ eV and approximately the same values $\tau=12$ ns and $\sigma=22$ ns at $E_0=10^{15}$ eV which should be regarded as reasonable estimates especially for the uncorrected data because the arrival time delay was calculated with respect to the arrival time of the fastest particle hitting the detector at the G/C-P experiment [31] while our estimates are given with respect to the arrival time of the flat light front and we did not take into account the nonrelativistic particles (e.g., the hadrons, the low energy muons, etc.) and other possible factors (e.g., the inaccuracy of the core location, etc.). Thus our calculation procedure suggested to calculate the average time delay τ and the disk thickness σ in giant showers at the distances above 0.5 km from the shower core are also capable of producing the reasonable estimates at shorter distances and much lower energies increasing the confidence that these simulations may be trusted as useful tools for the proposed new projects (e.g., the Auger project, the EAS-1000 project, etc.).

IV. CONCLUSION

In our endeavours to solve the mystery of cosmic rays with energies above the GZK cutoff, a full understanding of time-space structure of giant showers should be reached. Extensive calculations in the framework of some models of hadron interactions can shed more light on this complicated problem. With this goal in mind the calculations of time

delays and disk thickness for electrons, muons, and Cherenkov photons were carried out in terms of the QGS model both for vertical and inclined showers of energies 10^{17}, 10^{18}, 10^{19}, 10^{20}, and 10^{21} eV. The following time-space picture was found. When the vertical primary proton with a giant energy hits the atmosphere very energetic hadrons and gamma quanta are produced at a height of about 17 km which give very lower limits for time delays. Then at a height of about 5.5 km a cascade of low energy hadrons reaches its maximum and a muon disk (or better, a lens) starts its movement to the detector plane. About a 1.5 km lower Cherenkov photon disk is generated. At last at a height of 1–2 km or in the nearest vicinity of the detector plane electron cascade reaches its maximum and an electron disk is created. For this reason muons come first to the detector plane with a mean time delay of about 420 ns and a standard disk thickness of 250 ns at a core distance of 1000 m in a shower with energy of 10^{19} eV and then, about 30 ns later, Cherenkov photons follow in a time pulse with the 340 ns full width. Finally, electrons hit the detector plane with 1120 ns mean delay and 580 ns standard disk thickness. If the energy E_0 of the primary protons increases then the hadron-electron cascade reaches its maximum deeper in the atmosphere and all time parameters considerably increase. For strongly inclined showers the maximum of hadron-electron cascade is much higher in the atmosphere and all time parameters decrease. At distances above 1 km time delay and disk thickness may increase up to a few μs which is very important both for designing electronics of new shower arrays and interpreting experimental data. So the parameters of simple Linsley approximations for time delay and disk thickness depend on energy E_0 and zenith angle θ. Some simple approximations are suggested with the parameters presented in Tables I and III to display these dependencies.

Exact measurements of time pulses of muons, electrons, and Cherenkov photons are suggested to display rather precisely the hadron cascade development in the atmosphere showing maximum depths both for muons and electrons. This suggestion enables us to use these time data for estimations of shower core location and arrival direction, the energy and nature of primary particle in terms of some model of hadron interaction, or even this model testing.

ACKNOWLEDGMENTS

The authors wish to thank G. T. Zatsepin for helpful discussions. The Russian National Fund for Fundamental Investigations is thanked for support (Grant No. 95-02-056-a). We would also like to express our sincere thanks to K. Husimi for support and the Hitachi company for the possibility to use a Hitachi computer. Professor M. Nagano and Dr. K. Honda are sincerely thanked for a discussion of the AGASA data.

APPENDIX A: CALCULATION PROCEDURES

In principle the full Monte Carlo treatment of particles in cascades may be suggested (e.g., as in the CORSIKA code [32] and the COSMOS code [33]) with over a century of the amount of computing time required at 10^{20} eV [34]. One possibility to decrease the CPU time required is to follow all shower particles to a certain threshold energy and then to use libraries of precomputed subcascades to handle the subthreshold particles (e.g., as in the SIBYLL code [35]). Another approach is the ''thinning'' technique utilized in the MOCCA code [34] when only a fraction of the absurdly large number of low energy particles is followed with appropriate weight as in well known the Monte Carlo codes with ''weights.''

A promising approach consuming only a few minutes of CPU time at 10^{21} eV is the very simple hybrid algorithm suggested in Ref. [19]. To take into account the main fluctuations in the shower development the primary particle is followed by the full Monte Carlo code (as in the SIBYLL code [35] it is possible to use the full Monte Carlo method for all high energy particles) but a bulk of the low energy particles which contribute not so much into fluctuations of shower parameters contrary to the SIBYLL libraries method [35] are treated by the transport equation technique [19,20]. In the simplest case the depths x_i where the primary particle interacts with the nuclei in the atmosphere and the inelasticity coefficients k_i in each interaction are sampled by the Monte Carlo method in accordance with the QGS model [17]. At each depth x_i the average energy spectrum $P_{pr}(E,x_i)$ of pions (in simplest case only pions) produced by the primary particle is considered as the boundary condition for the transport equation

$$\frac{\partial P}{\partial x} = -\frac{B}{Ex}P - \frac{P}{\lambda(E)} + \int \frac{dE'}{\lambda(E')} P(E',x) f_{\pi\pi}(E',E), \tag{A1}$$

where B is the decay constant, $\lambda(E)$ is the mean interaction length for pions, and $f_{\pi\pi}(E',E)$ is the energy spectrum of pions produced by the pion with the energy E'. The solution of Eq. (A1) may be estimated by the recurrence procedure [20] through its integral form

$$\begin{aligned} P(E,x) = P_{pr} \exp\left(-(x-x_i)/\lambda(E) - \frac{\beta}{E} \ln \frac{x}{x_i} \right) \\ + \int_{x_i}^{x_0} d\xi \exp\left(-(x-\xi)/\lambda(E) - \frac{B}{E} \ln \frac{x}{\xi} \right) \\ \times \int_{E}^{E_0} dE' P(E',\xi) f_{\pi\pi}(E',E)/\lambda(E') \end{aligned} \tag{A2}$$

with an uncertainty of less than 1%. The generalization of this scheme for various kinds of particles is straightforward though as far as the time parameters are involved it seems to be not so important. Finally the solutions (A2) for neutral and charged pions may be considered as the source functions for the electron-photon and muon components.

APPENDIX B: THE RADIAL SPREAD OF MUONS ON THE ARRAY PLANE

The chain of successive generations of pions produced in the interactions with the atomic nuclei in the atmosphere

may sooner or later end by pion decay into a muon. Each newly produced pion with energy E deviates additionally from the shower core by the angle

$$\theta = p_\perp c/E, \tag{B1}$$

where $p_\perp$ is its transverse momentum determined by the parent pion with the energy E' and the distribution $\phi(E',p_\perp)dp_\perp$ and c is the speed of light. This deviation gives the radial spread on the array plane

$$r = \theta h(x), \tag{B2}$$

where $h(x)$ is the height of pion production which corresponds to the depth x.

Assuming the increase of $p_\perp$ as high as 0.04 GeV/c per decade of energy [36] and $h=20$ km one gets the spread $r = 1.5\times 10^{-7}$ m for the energy $E' = 10^{20}$ eV. So it is quite clear that only pions with the lowest possible energies contribute much to the spread of muons. Thus the small angle approximation may be used to estimate this spread, caused by successive generations of pions.

Multiplying Eq. (A1) by r^2 and inserting into the last term of Eq. (A1) the square of r defined by Eq. (B2) with the weight $\phi(E',p_\perp)dp_\perp$ (and integrating over $p_\perp$) one gets the following equation for the product $R = P(E,x)r^2$:

$$\frac{\partial R}{\partial x} = -\frac{R}{\lambda(E)} - \frac{B}{Ex}R + \int \frac{dE'}{\lambda(E')} P(E',x) f_{\pi\pi}(E',E) \times \int dp_\perp \left(\frac{p_\perp c}{E} h\right)^2 \phi(E',p_\perp). \tag{B3}$$

The solution of this equation $R(E,x)$ can be found by the formula which is analogous to Eq. (A2). So the system of equations (A1) and (B3) determines the mean square of the radial spread of pions on the array plane:

$$r^2(E,x,x_0) = R(E,x,x_0)/P(E,x). \tag{B4}$$

The total number $N_\mu(>E_{th},x_0)$ of muons with energies above the threshold $E_{\rm thr}$ at the observation level x_0 are estimated as

$$N_\mu = B\int_{x_i}^{x_0} \frac{dx}{x} \int_{E_{\rm thr}(x)}^{E_{\mu\,\max}} dE_\mu W(E_\mu,E_{\rm thr},x,x_0) \times \int_{E_{\min}(E_\mu)}^{E_{\max}(E_\mu)} \frac{dE}{E} D(E,E_\mu) P(E,x), \tag{B5}$$

where $P(E,x)$ is determined by Eq. (A2), the function $D(E,E_\mu)$ and limits $E_{\min}(E_\mu)$, $E_{\max}(E_\mu)$ are determined by the kinematics of the pion decay, and the function $W(E_\mu,E_{\rm thr},x,x_0)$ gives the probability for a muon with energy E_μ produced at the depth x to survive at the observation level x_0 with the energy not less than $E_{\rm thr}$ taking into account the ionization losses [37]. Finally, the average muon spread on the array plane can be estimated with the help of Eqs. (B4) and (B5) as

$$r_\mu^2 = \left(B\int_{x_i}^{x_0} \frac{dx}{x} \int_{E_{\rm thr}(x)}^{E_{\mu\,\max}} dE_\mu W \times \int_{E_{min}(E_\mu)}^{E_{\max}(E_\mu)} \frac{dE}{E} DPr^2(E,x,x_0) \right) \Big/ N_\mu. \tag{B6}$$

According to the small angle approximation it is possible to approximate this muon spread caused by many pion generations only by its parent pion spread but with the adjusted deflection function which may be assumed in the $p_\perp$ notation as

$$f_a(p_\perp) = p_\perp/p_0^2 \exp(-p_\perp/p_0). \tag{B7}$$

The only thing to do now is to estimate the value of p_0 in Eq. (B7). This can be done if we demand

$$r_\mu^2 = r_{\mu a}^2, \tag{B8}$$

where $r_{\mu a}^2$ is determined by Eq. (B6) with the replacement of $r^2(E,x,x_0)$ by

$$r_a^2(E,x) = \int dp_\perp f_a(p_\perp) \left(\frac{p_\perp c}{E} h(x)\right)^2, \tag{B9}$$

where the function f_a is given by Eq. (B7). The solution of Eq. (B8) gave

$$p_0 = 0.2 \quad \text{GeV}/c. \tag{B10}$$

The shape of the muon lateral structure function $\rho_\mu(r)$ found at the Yakutsk and AGASA arrays is well described by the adjusted function (B7) with this value of p_0 [38,39]. So the geometrical paths of muons and hence the time of movement may as well be described by the same approximation. Table IV shows the mean time delay τ and width σ for muons in the shower with the energy of 10^{20} eV calculated in terms of two assumptions when $p_0 = 0.2$ GeV/c = const and

$$p_0(E) = \begin{cases} 0.165 & \text{GeV}/c, \quad E \leqslant 10 \quad \text{GeV}, \\ 0.165 + 0.02 lg(E/10) & \text{GeV}/c, \quad E > 10 \quad \text{GeV}. \end{cases} \tag{B11}$$

It is seen from Table IV that there is no difference inside the uncertainties for the average time delay τ and approximately the 10% increase in the width σ in case of the assumption (B10).

The adjusted function (B7) describes the bulk of muons with transverse momenta below approximately 1 GeV/c well. Collider data [40,41] have shown that the transverse momentum distribution has a tail at larger $p_\perp$ values. To take into account this tail the power distribution was suggested [41]

$$\frac{1}{\sigma}\frac{d\sigma}{dp_\perp^2} = \frac{A}{(p_\perp + p_0)^\alpha}, \tag{B12}$$

TABLE IV. The average time delay τ and the width σ for suggestions (B10) and (B11).

R, m	τ, ns		σ, ns	
	p_0=const (B10)	p_0(E) (B11)	p_0=const (B10)	p_0(E) (B11)
100	15.0± 1.0	14.0± 1.0	17.0± 1.0	15.0± 1.0
300	71.0± 6.0	66.0± 5.0	62.0± 3.0	55.0± 2.0
600	200.0± 16.0	190.0± 15.0	140.0± 5.0	130.0± 5.0
1000	440.0± 34.0	410.0± 32.0	260.0± 8.0	230.0± 8.0
1500	810.0± 62.0	760.0± 60.0	400.0±11.0	360.0±10.0
2000	1300.0± 98.0	1200.0± 95.0	550.0±12.0	500.0±12.0
3000	2300.0±190.0	2100.0±190.0	860.0±11.0	770.0±13.0

where $p_0=1.3$ GeV/c, $\alpha=9.14$, and $A=$const. This $p_\perp$ distribution fits the data [40] well at $0.30<p_\perp<10$ GeV/c. We have used this distribution in the form

$$f(p_\perp)dp_\perp=\frac{(\alpha-1)(\alpha-2)}{p_0^2}\left(\frac{p_0}{p_0+p_\perp}\right)^2 p_\perp dp_\perp, \tag{B13}$$

to find out the contribution of the power tail to the muon density and time parameters. We took $p_0=1.2293$ to adjust the average $p_\perp$ value to 0.4 GeV/c. Table V displays densities ρ_μ, average time delays τ and time front widths σ for muons in the vertical shower with an energy of 10^{20} eV at different radial distances R calculated in terms of Eqs. (B7) and (B13). Table V shows that at radial distances above the power $p_\perp$ distribution (B13) gives a considerably larger muon density (by a factor of 1.6) though time parameters τ and σ are not effected much (less than 30%). Inside the circle with the radius of 2000 m the approximation (B7) produces reasonable results. As far as time parameters τ and σ are concerned this approximation is not so bad even at larger distances. Thus Table V may be used as a guide how to correct calculated time parameters at distances above 2000–3000 m.

APPENDIX C: ELECTRON AND MUON TIME PULSES

To interpret the experimental data [29,30] in terms of the QGS model we have to be able to calculate the time pulses for both electrons and muons. With the help of the effective function $f_a(p_\perp)$ introduced in Appendix B it is straightforward to estimate the contribution to the muon density from depth interval $x \div x+dx$ at fixed distance R from the shower core as

$$\rho_\mu(R,x,E)=\frac{B}{Ex}PW\exp\left(-\frac{RE}{cp_0h}\right)\left(\frac{E}{p_0c}\right)^2\Big/\, h^2, \tag{C1}$$

where the probability W, the pion spectrum P, and other values were defined above (see Appendix B). The height $h=h(x)$ corresponds to the depth x in the atmosphere. Assuming the simplest estimate for time t as

$$t=h[\sqrt{1+(R/h)^2}-1], \tag{C2}$$

it is possible to calculate the depths $x_i[h(t_i)]$ and $x_{i+1}[h(t_{i+1})]$ which correspond to the times t_i and t_{i+1}. So the muon time pulse may be estimated with help of the formula

$$\delta\rho_\mu(R,\delta t)=\frac{1}{\delta t}\int_{x_i}^{x_{i+1}}dx\int dE\rho_\mu(R,x,E), \tag{C3}$$

where the difference $\delta t=t_{i+1}-t_i$ determinates the time bin. It was suggested that all muons are moving with the speed of light.

As for the electron time pulse it was assumed that in any individual electron-photon shower generated by a gamma quantum produced in neutral pion decays the angle distribution of electrons at depth x_i is given by the Gaussian law

TABLE V. The muon density ρ_μ, the average time delay τ, and the width σ for approximations (B7) and (B13).

R, m	ρ_μ, m^{-2}		τ, ns		σ, ns	
	(B13)	(B7)	(B13)	(B7)	(B13)	(B7)
100	1.4×10^{3}	1.4×10^{3}	1.5×10^{1}	1.5×10^{1}	1.7×10^{1}	1.7×10^{1}
300	1.7×10^{2}	1.8×10^{2}	7.0×10^{1}	7.1×10^{1}	6.4×10^{1}	6.2×10^{1}
600	3.0×10^{1}	3.3×10^{1}	2.1×10^{2}	2.0×10^{2}	1.5×10^{2}	1.4×10^{2}
1000	6.3×10^{0}	6.8×10^{0}	4.6×10^{2}	4.4×10^{2}	2.9×10^{2}	2.6×10^{2}
1500	1.5×10^{0}	1.5×10^{0}	8.8×10^{2}	8.1×10^{2}	4.9×10^{2}	4.0×10^{2}
2000	4.6×10^{-1}	4.0×10^{-1}	1.4×10^{3}	1.3×10^{3}	7.0×10^{2}	5.5×10^{2}
3000	7.3×10^{-1}	4.5×10^{-1}	2.7×10^{3}	2.3×10^{3}	1.1×10^{3}	8.6×10^{2}

$$f(\theta)d\theta=\frac{1}{\sqrt{2\pi\theta_e^2(x_c)}}\exp[-\theta^2/2\theta_e^2(x_c)]d\theta, \quad \text{(C4)}$$

where x_c is defined in the cascade units and θ_e^2 is a dispersion. The simplest approximation of calculations [42] was used for this dispersion:

$$\theta_e(x_c)=\begin{cases}0.005x_c & \text{for } x_c\leqslant x_{\max},\\ 0.005x_{\max}+0.0001(x_c-x_{\max}) & \text{for } x_c>x_{\max}.\end{cases} \quad \text{(C5)}$$

Then with the help of the angle θ determination

$$tg\,\theta=R/h(x_c) \quad \text{(C6)}$$

it is possible to suggest the weight function (WF):

$$\mathrm{WF}(x_c)=CN_e(x_i)f(\theta)D(h_i,R), \quad \text{(C7)}$$

where the depth x_i is determined by Eq. (C2) for corresponding value of t_i, the electron number $N_e(x_c)$ is taken in the NKG approximation, the function $D(h_i,R)$ is determined by transformations of the differential $d\theta$ from Eqs. (C6) and (C2),

$$D(h_i,R)=\{[R/(ct_i)]^2+1\}/(R^2+h_i^2), \quad \text{(C8)}$$

and the normalization constant C is determined by the integral

$$\int_0^\infty \mathrm{WF}(x_c)dx_c=1. \quad \text{(C9)}$$

Finally the electron time pulse in gamma induced shower may be estimated as

$$\delta\rho_e(R,\delta t)=\frac{1}{\delta t}\int_{x_i}^{x_{i+1}}\mathrm{WF}(x_c)\rho_e(R)dx_c, \quad \text{(C10)}$$

where the difference $\delta t=t_{i+1}-t_i$ is the time bin, the depths x_i and x_{i+1} are determined by Eq. (C2) through the height h and time t, and the electron density $\rho_e(R)$ at radial distance R is taken in the NKG or in the modified NKG approximations. At last the sum of the pulses (C10) over all gamma quanta produced in the proton induced shower constitutes the total electron pulse.

APPENDIX D: MAIN FEATURES OF THE QGS MODEL

The QGS model have been used mainly in the approximation form [43] with the parameter $\delta=0.14$ [17]. The inelastic cross section of the interactions of the primary protons with atomic nuclei in the atmosphere increases at the rate of 2.7% per decade of energy from the value of 270 mb at energy 250 GeV. The average coefficient of inelasticity increases also from 0.6 by the value of 0.0047 per every decade of energy. The inelastic cross section of pion interactions are approximately by the factor of 1.35 less than for protons an 200 GeV and the difference decreases at higher energies. The inclusive spectra of secondary particles are taken in the form when the scaling in the fragmentation region is slightly violated. Thus many model parameters are close to the predictions of the QGSJET model [44] except the semihard processes which were not taken into account.

TABLE VI. Shower maximum positions $x_{\max}$ in g cm^{-2} in the proton showers.

Code	E_0, eV			
	10^{18}	10^{19}	10^{20}	10^{21}
mocca92 [55]	810	875	945	
SIBYLL [55]	765	820	880	
QGSJET [44]	728	787	850	
QGS [56]	725	784	849	895

The photoproduction of pions is also not included though Ref. [45] states that it is of importance at the muon threshold energy of 0.3 GeV but the fraction of photoproduced pions decreases to the 10% level and even less at the threshold energies above 1 GeV. The scaling model used in Ref. [45] decreases severely (by several times) the fraction of muons produced via the usual pion decays. Besides the muon threshold energy $E_\mu=0.5$ GeV for the vertical showers in case of the AGASA array should be enlarged by the value of 0.8 GeV lost by muons due to the ionization processes and on average by a factor of 1.3 to take into account the neutrino energy. Thus pions with energies above 1.7 GeV should be mainly considered in our case. At such energies the cross section for photoproduction is nearly the value of 0.14 mb [46]. Assuming this cross section we have approximately found the fraction of photoproduced muons not larger than a few per cent. Our estimate seems to agree with the conclusions in Refs. [47,48]. More sophisticated calculations may be suggested to treat the photoproduction problem in detail both at low energies and at the upper end of the energy spectrum of the primary particles in a separate paper to take into account the very interesting possibility [49] that gamma rays may mask the ''black body cutoff'' in the cosmic ray spectrum. The data [46,50,51] and the calculations [52] ruled out the possibility of the essential increase of the photoproduction cross section [53,54] at energies up to 10^{16} eV (the estimate is less than 0.22 mb) but it needs a special consideration at much higher energies.

Nevertheless it is not so difficult to predict some basic consequences of the drastic increase of the photoproduction cross section at energies around 10^{19} eV. In this case photons would interact with atomic nuclei in the atmosphere similar to hadrons contributing to some extra production pions and kaons. Thus a larger fraction of the primary particle energy would go to muons. But the height of this extra production would be only negligibly higher in the atmosphere comparing with the usual hadron cascade development. So the result would be the noticeable increase in the muon density (especially in the ratio of muons to electrons) and almost no effect on the average time delay and the time front width of muons. The time parameters for electrons would be slightly decreasing because the shower maximum position tends to be higher in the atmosphere due to consid-

erable decreasing of the photon energies which go into the electron-photon cascades.

It is of interest to compare some basic shower parameters estimated in terms of different interaction models. Table VI displays the average shower maximum positions $x_{\max}$ in $g\,\mathrm{cm}^{-2}$ for various energies. At energies above 10^{19} eV the neutral pion interactions and the LPM effect decrease the elongation rate (ER) [57] up to 46 $\mathrm{g\,cm}^{-2}$ at 10^{21} eV.

It is well known that the size $N_{\max}$ at the shower maximum does not depend much on the interaction model. Our calculations [56] gave that the ratio $N_{\max}/E_0$ is decreasing from 0.76 GeV^{-1} at 10^{18} eV down to 0.71 GeV^{-1} at 10^{20} eV and to 0.65 GeV^{-1} at 10^{21} eV due to the LPM effect. So as is seen from Table V the QGS model [17] we have used admits the higher rate of the primary particle energy dissipation compared with the MOCCA and the SIBYLL codes [55].

[1] J. Linsley, Phys. Rev. Lett. **10**, 146 (1963).
[2] D.M. Edge *et al.*, J. Phys. A **6**, 1612 (1973).
[3] G.Brooke *et al.*, in *Proceedings of the 19th International Cosmic Ray Conference*, La Jolla, CA, 1985, edited by F. C. Jones *et al.* (Goddard Space Flight Center, Greenbelt, MD), Vol. 2, p. 150.
[4] C.J. Bell *et al.*, J. Phys. A **7**, 990 (1974).
[5] L. Horton *et al.*, in *Proceedings of the 19th International Cosmic Ray Conference*, La Jolla, CA, 1985, edited by F.C. Jones *et al.* (Goddard Space Flight Center, Greenbelt, MD), Vol. 9, p. 499.
[6] M.A. Markov, Report No. P-0208, Inst. Nucl. Research Acad. Sci. USSR, Moscow, 1981.
[7] C.T. Hill *et al.*, Phys. Rev. D **36**, 1007 (1987).
[8] K. Greisen, Phys. Rev. Lett. **2**, 748 (1966).
[9] G.T. Zatsepin and V.A. Kuzmin, Pis'ma Zh. Eksp. Teor. Fiz. **4**, 114 (1966) [JETP Lett. **4**, 78 (1966)].
[10] N.N. Efimov *et al.*, in *Proceedings of the International Workshop on Astrophysical Aspects of the Most Energetic Cosmic Rays*, Kofu, Japan, 1990, edited by M. Nagano and F. Takahara (World Scientific, Singapore, 1991), p. 20.
[11] N. Hayashida *et al.*, Phys. Rev. Lett. **73**, 3491 (1994).
[12] D.J. Bird *et al.*, Astrophys. J. **441**, 144 (1995).
[13] V.S. Berezinsky and S.I. Grigorieva, Astron. Astrophys. **199**, 1 (1988); **210**, 462 (1988).
[14] G.B. Khristiansen *et al.*, Nucl. Phys. B (Proc. Suppl.) **28B**, 40 (1992).
[15] J.C. Cronin *et al.*, University of Chicago Report No. EHI 92-08, 1992.
[16] M. Teshima *et al.*, in *Proceedings of the RIKEN International Workshop on Electromagnetic and Nuclear Cascade Phenomena in High and Extremely High Energies*, Tokyo, Japan, 1993, edited by M. Ishihara and A. Misaki (The Institute of Physical and Chemical Research, Wako, 1993), p. 135.
[17] A.B. Kaidalov, K.A. Ter-Martirosyan, and Yu. M. Shabelsky, Yad. Fiz. **43**, 1282 (1986) [Sov. J. Nucl. Phys. **43**, 822 (1986)].
[18] A.B. Migdal, Phys. Rev. **103**, 1811 (1956).
[19] L.G. Dedenko, Can. J. Phys. **46**, 178 (1968).
[20] L.G. Dedenko, in *Proceedings of the 9th International Cosmic Ray Conference*, London, 1966, edited by A. C. Stickland (The Institute of Physics and Physical Society, London, 1965), Vol. 2, p. 662.
[21] S. Mikocki *et al.*, in *Proceedings of the 20th International Cosmic Ray Conference*, Moscow, 1987, edited by V.A. Kozyarivsky *et al.* (Nauka, Moscow, 1987), Vol. 6, p. 75.
[22] K. Greisen, *Progress in Cosmic Ray Physics III*, edited by J.G. Wilson (North-Holland, Amsterdam, 1956), p. 26.
[23] A.M. Anokhina *et al.*, Astrophys. Space Sci. **209**, 19 (1993).
[24] J. Linsley, report, 1983 (unpublished); in [3], Vol. 7, p. 359.
[25] M. Teshima *et al.*, J. Phys. G **12**, 1097 (1986).
[26] V.B. Atrashkevich *et al.*, in [21], Vol. 6, p. 63.
[27] A.A. Belyaev *et al.*, *Electron-Photon Cascades in Cosmic Rays at Super High Energies* (Nauka, Moscow, 1980).
[28] V.B. Atrashkevich *et al.*, J. Phys. G **23**, 237 (1997).
[29] K. Honda *et al.*, Phys. Rev. D **56**, 3833 (1997).
[30] EAS-TOP Collaboration, M. Aglietta *et al.*, INFN Report No. LNGS-93/77, Gran Sasso, 1993.
[31] M. Ambrosio *et al.*, Astropart. Phys. **7**, 329 (1997).
[32] J.N. Capdevielle *et al.*, J. Phys. G **15**, 909 (1989).
[33] K. Kasahara, in *Proceedings of the 24th International Cosmic Ray Conference*, Roma, Italy, 1995 (Istituto Nazionale Fisica Nucleare, Rome, 1995), Vol. 1, p. 399.
[34] A.M. Hillas, Nucl. Phys. B (Proc. Suppl.) **52B**, 29 (1997).
[35] R. Fletcher *et al.*, Phys. Rev. D **50**, 5710 (1994).
[36] T. Alexopoulos *et al.*, Phys. Rev. D **48**, 984 (1993).
[37] B. Rossi, *High Energy Particles* (Prentice-Hall, Englewood Cliffs, NJ, 1952).
[38] A.M. Anokhina *et al.*, Phys. At. Nucl. **60**, 230 (1997).
[39] N. Hayashida *et al.*, in *Proceedings of the 25th International Cosmic Ray Conference*, Durban, South Africa, 1997, edited by M. S. Potgieter, B. C. Raubenheimer, and D. J. van der Walt (Potchefstroomse Universiteit, Durban, 1997), Vol. 6, p. 241.
[40] UA1 Collaboration, G. Arnison *et al.*, Nucl. Phys. **B291**, 445 (1987).
[41] G.J. Alner *et al.*, Nucl. Phys. **B291**, 445 (1987).
[42] L.G. Dedenko *et al.*, in *Proceedings of the FSU Cosmic Ray Conference of Kazahstan State University*, Alma-Ata, 1989 (Kazahstan State University, Alma-Ata, Kazahstan, 1989), Vol. 2, p. 3 (in Russian).
[43] N.N. Kalmykov *et al.*, Yad. Fiz. **41**, 947 (1985) [Sov. J. Nucl. Phys. **41**, 608 (1985)].
[44] N.N. Kalmykov *et al.*, Nucl. Phys. B (Proc. Suppl.) **52B**, 17 (1997).
[45] T.J.L. McComb *et al.*, J. Phys. G **5**, 1613 (1979).
[46] Particle Data Group, R.M. Barnett *et al.*, Phys. Rev. D **54**, 1 (1996), p. 198.
[47] F. Halzen *et al.*, in *Proceedings of the 21th International Cosmic Ray Conference*, Adelaide, Australia, 1990, edited by R. J. Protheroe (Graphic Services, Northfield, South Australia, 1990), Vol. 9, p. 142.

[48] T. Stanev *et al.*, Phys. Rev. D **32**, 1244 (1985).
[49] F.A. Aharonian *et al.*, Astrophys. Space Sci. **167**, 111 (1990).
[50] ZEUS Collaboration, M. Derrick *et al.*, Z. Phys. C **63**, 391 (1994).
[51] H1 Collaboration, S. Aid *et al.*, Z. Phys. C **69**, 27 (1995).
[52] R. Engel *et al.*, Phys. Rev. D **55**, 6957 (1997).
[53] R.S. Fletcher *et al.*, Phys. Rev. D **45**, 377 (1992).
[54] R.S. Fletcher *et al.*, Phys. Rev. D **45**, 3279 (1992).
[55] T.K. Gaisser *et al.*, in [39], Vol. 6, p. 281.
[56] L.G. Dedenko, in [16], p. 231.
[57] J. Linsley, in *Proceedings of the 15th International Cosmic Ray Conference*, Plovdiv, Bulgaria, 1977 (Bulgarian Academy of Science, Provdiv, Bulgaria, 1977), Vol. 12, p. 89.